

Variational study of a two-level system coupled to a harmonic oscillator in an ultrastrong-coupling regime

Myung-Joong Hwang¹ and Mahn-Soo Choi^{2,*}¹*Department of Physics, Pohang University of Science and Technology, Pohang 790-784, Korea*²*Department of Physics, Korea University, Seoul 136-713, Korea*

(Received 10 June 2010; published 30 August 2010)

The nonclassical behavior of a two-level system coupled to a harmonic oscillator is investigated in the ultrastrong coupling regime. We revisit the variational solution of the ground state and find that the existing solutions do not account accurately for nonclassical effects such as squeezing. We suggest a trial wave function and demonstrate that it has an excellent accuracy for the quantum correlation effects as well as for the energy.

DOI: [10.1103/PhysRevA.82.025802](https://doi.org/10.1103/PhysRevA.82.025802)

PACS number(s): 42.50.Pq, 42.50.Dv, 85.25.Cp

Introduction. A two-level system interacting with a harmonic oscillator appears in various fields in physics, ranging from an atom coupled to a photon inside of an optical cavity [1] to a Cooper-pair box coupled to a nanomechanical oscillator [2]. A theoretical model that describes the system is expressed by the Hamiltonian

$$H = \omega_0 a^\dagger a + \frac{1}{2} \Omega \sigma_z - \lambda (a + a^\dagger) \sigma_x + \lambda^2, \quad (1)$$

where ω_0 is the energy of the oscillator, Ω is the spin level splitting, and λ is the coupling strength. The Pauli matrices characterize the two-level system, while a and a^\dagger denote the boson operators.

The Hamiltonian (1) reveals completely different physics at different scales of ω_0 , Ω , and λ . For example, a cavity quantum electrodynamics (QED) operates in a regime where $\lambda, |\omega_0 - \Omega| \ll \omega_0, \Omega$, under which the counter-rotating terms of the Hamiltonian (1), $a^\dagger \sigma^+$ and $a \sigma^-$, can be neglected. Within this rotating wave approximation, the model reduces to a Jaynes-Cummings model and is solvable exactly [3]. The ground state is a simple direct product of the ground states of the oscillator and the spin. In contrast, in the so-called *ultrastrong coupling* regime ($\Omega \gg \omega_0$ and $\lambda \sim \sqrt{\Omega \omega_0}$), interesting quantum effects arise in the ground state; the two-level system and the oscillator are entangled. The degree of entanglement increases monotonically as a function of the *dimensionless coupling constant* $g \equiv 2\lambda/\sqrt{\Omega \omega_0}$. It also shows a squeezing effect [4]; that is, the variance of momentum quadrature in the ground state becomes smaller than the uncertainty minimum [5–7]. Hereafter, we set $\omega_0 = 1$ for simplicity.

The aforementioned ultrastrong regime has recently attracted much attention because of the possibility of realizing it experimentally in a circuit QED system [7–10]. Furthermore, as rather a theoretical problem, the ultrastrong coupling regime when Ω becomes ∞ has also been studied extensively because it shows a phase-transition-like behavior in the entanglement between the oscillator and the qubit in the ground state [11–16].

In this paper, we develop a variational ground state. The variational method had already been used for the Hamiltonian (1). A displaced coherent state for $g \gg 1$, a displaced squeezed state for $g \ll 1$ [17], and a superposition of two coherent states

for $g \simeq 1$ [18,19] have been suggested as variational ground states, respectively. The accuracy of the suggested variational states was reasonable for the ground-state energy [17–19]. However, we find that the variational states suggested in previous work [18,19] underestimate the squeezing effect significantly in the intermediate regime ($g \simeq 1$); see Figs. 2(b) and 2(e). The failure becomes more pronounced as Ω increases.

This observation implies that an energy-optimized variational wave function does not necessarily capture all the quantum correlation effects in the true ground state of the system. In this paper, we suggest a new variational ground state which captures the squeezing effect accurately.

First, we derive an equivalent model with only a boson degrees of freedom, followed by a derivation of an effective classical Hamiltonian by utilizing a parity symmetry in the model [20]. We observe that this effective classical Hamiltonian shows bifurcation around $g = 1$, which is consistent with the observation in Refs. [12] and [14] based on a classical model of Eq. (1) and gives a qualitative account of the properties of the ground state. We then suggest a superposition of two displaced-squeezed states as a trial wave function and demonstrate that it can predict the squeezing effect accurately. This shows that a deformation of each superposed wave packet is crucial to the squeezing effect of the ground state. We also discuss the drastic change in the degree of entanglement as g varies across $g = 1$ when $\Omega \rightarrow \infty$.

Effective Hamiltonian. The model (1) has a useful symmetry. If $|n', \sigma'\rangle = H|n, \sigma\rangle$, then $n' + \sigma' \pmod{2} = n + \sigma \pmod{2}$, where $|n, \sigma\rangle \equiv |n\rangle \otimes |\sigma\rangle$, $|n\rangle$ ($n = 0, 1, 2, \dots$) is the boson number state, $a^\dagger a |n\rangle = n |n\rangle$, and $|\sigma\rangle$ ($\sigma = \pm 1$) is the spin state, $\sigma_z |\sigma\rangle = \sigma |\sigma\rangle$. We further stress this symmetry by introducing a generalized “parity” operator:

$$\Pi = \exp(-i\pi a^\dagger a) \sigma_z. \quad (2)$$

Clearly, the Hamiltonian (1) is invariant under transformation described by Π , $[H, \Pi] = 0$. The operator Π has two eigenvalues ± 1 , and corresponding eigenstates are given by

$$|\varphi_n^\sigma\rangle \equiv \frac{(a^\dagger)^n \sigma_z^n}{\sqrt{n!}} |0, \sigma\rangle \quad (\sigma = \pm 1). \quad (3)$$

Namely, $\Pi|\varphi_n^\pm\rangle = \pm|\varphi_n^\pm\rangle$. The Hilbert space can be decomposed into a direct sum $\mathcal{E} = \mathcal{E}_+ \oplus \mathcal{E}_-$ of two subspaces \mathcal{E}_\pm spanned by $|\varphi_n^\pm\rangle$, respectively. Accordingly, the Hamiltonian

*choims@korea.ac.kr

can also be written as $H = H_+ \oplus H_-$, where H_{\pm} belongs to the subspace \mathcal{E}_{\pm} , and the partition function $Z \equiv \text{Tr}[e^{-\beta H}]$ as $Z = Z_+ + Z_-$, where $Z_{\pm} \equiv \text{Tr}[e^{-\beta H_{\pm}}]$.

Now we make the key observation, suggested in the expression for the parity eigenstates in Eq. (3), that the combination $a^{\dagger}\sigma_x$ behaves like a boson operator within each subspace \mathcal{E}_{\pm} . To show this rigorously, we first take a drone-fermion representation [21] of spin $\sigma_z = 2f^{\dagger}f - 1$ and $\sigma_+ = \sigma_-^{\dagger} = f^{\dagger}(d + d^{\dagger})$, where f and d are fermion operators. We then define a new boson operator $b^{\dagger} = a^{\dagger}(f^{\dagger} - f)(d + d^{\dagger})$, which satisfies $[b, b^{\dagger}] = 1$. The parity basis states are then written as

$$|\varphi_n^{\sigma}\rangle = \frac{(b^{\dagger})^n}{\sqrt{n!}}|0, \sigma\rangle, \quad (4)$$

where $|0, \sigma\rangle$ serves as the ‘‘vacuum’’ of the new boson operator b within \mathcal{E}_{σ} . It is now clear that the sub-block Hamiltonians H_{\pm} can be rewritten solely in terms of the boson operator b as

$$H_{\pm} = (b^{\dagger} - \lambda)(b - \lambda) \pm \frac{1}{2}\Omega \cos(\pi b^{\dagger}b). \quad (5)$$

The same expression was also derived in Ref. [20] using a canonical transformation. Having only a boson field, expression (5) allows us to compare the model directly with the corresponding classical system by deriving the classical effective potential.

To get a classical effective potential, we express the partition functions Z_{\pm} in terms of a functional integration [22]. $Z_{\pm} = \int \mathcal{D}[\phi^*(\tau), \phi(\tau)] \exp(-S_{\pm})$, with the action defined by

$$S_{\pm} = \int_0^{\beta} d\tau [\phi^* \partial_{\tau} \phi + (\phi^* - \lambda)(\phi - \lambda) \pm \frac{1}{2}\Omega e^{-2\phi^* \phi}], \quad (6)$$

where β is the inverse temperature and ∂_{τ} denotes the partial derivative with respect to the imaginary time τ . Making a change in variables, $p = (\phi^* + \phi)/\sqrt{2}$ and $x = i(\phi^* - \phi)/\sqrt{2}$, we can rewrite the functional integrals as $Z_{\pm} = \int \mathcal{D}[x(\tau), p(\tau)] \exp(-S_{\pm})$, with

$$S_{\pm} = \int_0^{\beta} d\tau [-ip \partial_{\tau} x + H_{\text{cl}}^{\pm}(x, p)]. \quad (7)$$

Here $H_{\text{cl}}^{\pm}(x, p)$ is the effective classical Hamiltonian defined by

$$H_{\text{cl}}^{\pm}(x, p) = \frac{1}{2}[(x - \sqrt{2}\lambda)^2 + p^2] \pm \frac{1}{2}\Omega e^{-(x^2 + p^2)}. \quad (8)$$

The potential profile is depicted in Fig. 1 for both $\Omega = 10$ and $\Omega = 10^5$. For $g \ll 1$, the classical potential has one local minimum and is highly anharmonic, illustrating why

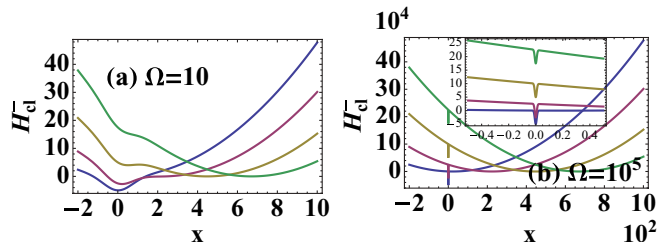


FIG. 1. (Color online) Profile of $H_{\text{cl}}^-(x, 0)$: (a) for $\Omega = 10$ and (b) for $\Omega = 10^5$. Different curves correspond to $g = 0.1, 1, 2, 3$ (from bottom to top). The inset in (b) zooms in on the region around $x = 0$.

a squeezed state localized around $x = 0$ is a good variational solution in this regime. As g approaches the critical value, 1, it shows a bifurcation of its local minimum as in the corresponding classical system. As g increases further, its local minimum around the origin disappears and a single local minimum develops at $x \sim g\sqrt{\Omega}/2$. This is also consistent with the fact that the coherent state is a good approximation in this regime.

Variational solutions. We have seen from the effective classical potential that the model in Eq. (1) shows highly nontrivial behaviors in the regime $g \sim 1$. Now we investigate this regime more closely in terms of variational wave functions. To test the accuracy of a given trial wave function, we examine not only the energy but also the quantum correlation effects such as squeezing and spin-oscillator entanglement. We characterize the squeezing effect with the momentum variance ΔP and the spin-oscillator entanglement with *tangle* [23] defined by $\tau = 2[1 - \text{Tr}(\rho_s^2)]$, where ρ_s is a reduced density matrix of the two-level system. We test the variational solution for two cases, $\Omega = 10$ and $\Omega = 10^5$, by comparing it with the exact solution. The exact solution is numerically calculated by the exact diagonalization method [24], where a sufficient number of Fock basis states $|n\rangle$ (typically 300 states for $\Omega = 10$ and 3000 states for $\Omega = 10^5$) is kept until the desired accuracy is achieved.

In Refs. [17] and [19], a superposition of two displaced coherent states was suggested as a trial wave function:

$$|\psi(\alpha_1, \alpha_2, t)\rangle = (1 - t)|\alpha_1\rangle + t|\alpha_2\rangle, \quad (9)$$

where $|\alpha\rangle = D(\alpha)|0\rangle$, with $D(\alpha) = \exp[\alpha(b^{\dagger} - b)]$. Hereafter we refer to the trial wave function in Eq. (9) as the *double coherent state* (DCS). It shows a reasonable accuracy for the energy (with an error of about 1%) in the intermediate regime [see Figs. 2(a) and 2(e)]. Although neither our effective classical potential nor a bifurcation of fixed point in the corresponding classical system can give a quantitative account of the ground state, the fact that a superposition of two wave packets is a good approximation for the ground state is consistent with the classical observations of bifurcation.

However, as shown in Figs. 2(b) and 2(f), the degree of entanglement between the spin and the oscillator exhibits relatively larger deviations, especially for large Ω .

The poor accuracy of the variational solution in Eq. (9) is even more noticeable (more than 30%) on the momentum variance ΔP of the ground state. For both $\Omega = 10$ and $\Omega = 10^5$, the squeezing effect is considerably underestimated in this scheme. Moreover, for the true adiabatic regime, the variational solution predicts that the squeezing effect suddenly disappears when g becomes larger than 1.

We can understand the reason for the failure by looking at the optimized variational parameters shown in Fig. 3(e). If $g \ll 1$, the variational states are optimized at $\alpha_1 = -\alpha_2 \sim g\sqrt{\Omega}/2$. In this case, there is a considerable overlap between two coherent states which results in the squeezing effect. On the contrary, when g becomes larger than 1, the variational parameter abruptly changes, and the value for α_1 and α_2 becomes an order of 10 or 100, still having opposite signs from each other. Then the overlap between two coherent states vanishes and cannot give the squeezing effect. This observation leads us to conclude that a deformation of individual wave

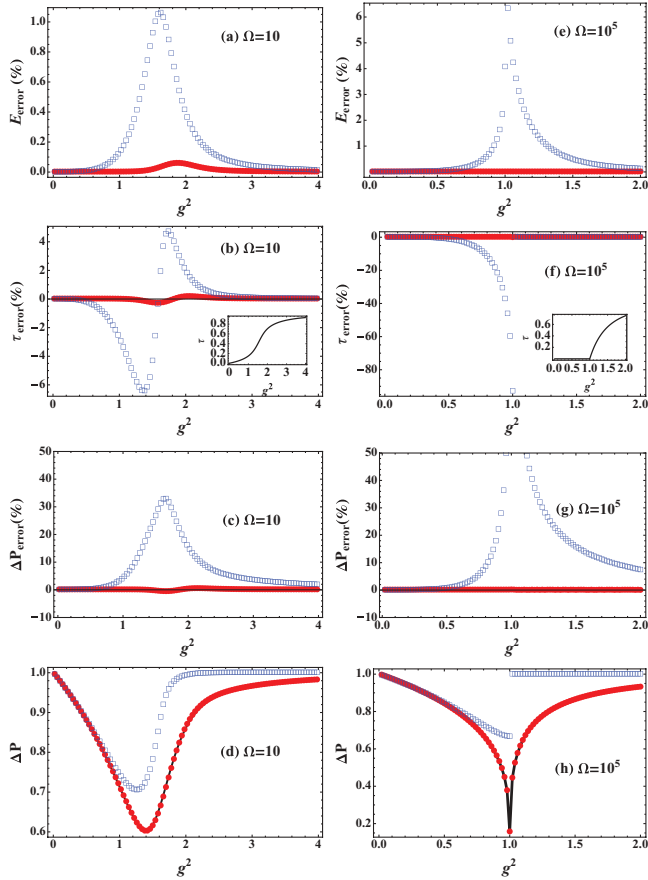


FIG. 2. (Color online) Comparison of variational solutions with the exact solution. The open (blue) square represents the DCS wave function, while the filled (red) circle indicates the DSS wave function. (a, e) Error in the energy with respect to the exact energy. (b, f) Error in the tangle. (c, g) Error in the momentum variance. (d, h) Momentum variance of the ground state; the solid (black) line indicates the exact solution.

packets is considerable in the true ground state, and unless the effect is taken into account in the trial wave function, the squeezing effect is inevitably underestimated.

Motivated by the preceding observation, we propose a superposition of two displaced-squeezed states as a trial wave function,

$$|\psi(r_1, \alpha_1, r_2, \alpha_2, t)\rangle = (1-t)|r_1, \alpha_1\rangle + t|r_2, \alpha_2\rangle, \quad (10)$$

where $|r, \alpha\rangle$ denotes the displaced-squeezed state [25] defined by $|r, \alpha\rangle = S(r)|\alpha\rangle$ with $S(r) = \exp[(rb^\dagger b^\dagger - r^*bb)/2]$. We refer to the wave function in Eq. (10) as the *double squeezed state* (DSS). Without a loss of generality, the displacement parameter α and the squeezing parameter r are assumed to be real.

The variational parameters r_1 , α_1 , r_2 , α_2 , and t are determined by minimizing the energy $E(r_1, \alpha_1, r_2, \alpha_2, t) = \langle \psi | H_- | \psi \rangle / \langle \psi | \psi \rangle$. It includes two direct terms,

$$\langle r_j, \alpha_j | H_- | r_j, \alpha_j \rangle = \sinh^2 r_j + (\lambda - \alpha_j e^{r_j})^2 - \frac{\Omega}{2} e^{-2\alpha_j^2}, \quad (11)$$

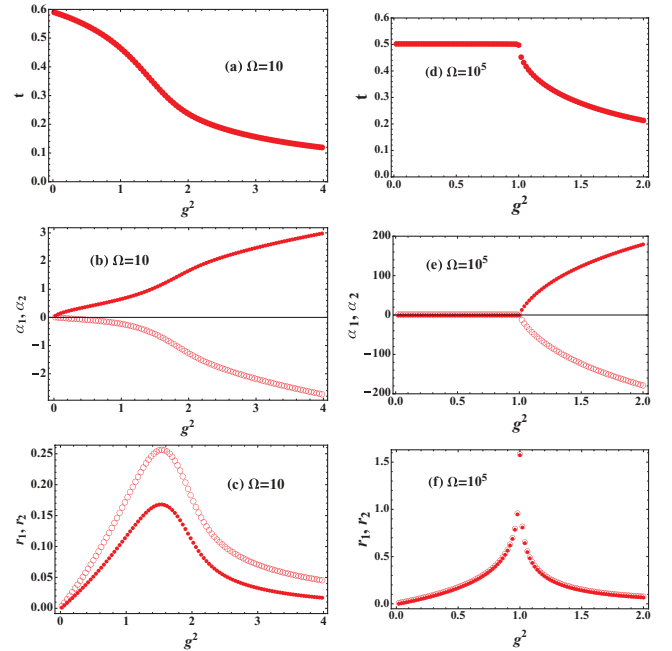


FIG. 3. (Color online) Optimized variational parameters for the double squeezed state [Eq. (9)] for $\Omega = 10$ (a–c) and for $\Omega = 10^5$ (d–f). The variational parameters for the double coherent state [Eq. (10)] are qualitatively similar (not shown) except for $r_1 = r_2 = 0$. (a, d) Relative weight t in the superposition. (b, e) Displacement parameters α_1 and α_2 . (c, f) Squeezing parameters r_1 and r_2 .

for $j = 1, 2$, and a cross term,

$$\begin{aligned} & \frac{\langle r_1, \alpha_1 | H_1 | r_2, \alpha_2 \rangle}{\langle r_1, \alpha_1 | r_2, \alpha_2 \rangle} \\ &= \text{sech}(r_1 - r_2) \sinh r_1 \sinh r_2 \\ &+ [\lambda - \text{sech}(r_1 - r_2)(\alpha_1 \cosh r_2 + \alpha_2 \sinh r_1)] \\ &\times [\lambda - \text{sech}(r_1 - r_2)(\alpha_1 \sinh r_2 + \alpha_2 \cosh r_1)] \\ &- \frac{1}{2} \Omega \exp[-2\text{sech}(r_1 - r_2)\alpha_1 \alpha_2], \end{aligned} \quad (12)$$

where

$$\begin{aligned} & \langle r_1, \alpha_1 | r_2, \alpha_2 \rangle \\ &= \frac{\exp[\alpha_1 \alpha_2 \text{sech}(r_1 - r_2)]}{\sqrt{\cosh(r_1 - r_2)}} \\ &\times \exp\left[-\frac{(\alpha_1^2 + \alpha_2^2) + (\alpha_1^2 - \alpha_2^2) \tanh(r_1 - r_2)}{2}\right]. \end{aligned} \quad (13)$$

The optimum variational parameters r_1 , r_2 , α_1 , α_2 , and t thus determined are plotted as a function of g in Fig. 3. The squeezing parameters r_1 and r_2 of the individual wave packets in the DSS are indeed large in the regime $g \simeq 1$, where the DCS variational solution changes abruptly. This is consistent with our prediction.

Using this variational solution, we calculate the momentum variance. The variance ΔP of the momentum $P = i(b^\dagger - b)$ is given by $\Delta P = \langle \psi | P^2 | \psi \rangle / \langle \psi | \psi \rangle$, as in our case $\langle \psi | P | \psi \rangle = 0$. The direct terms and cross term are, respectively, given by $\langle r_j, \alpha_j | P^2 | r_j, \alpha_j \rangle = e^{-2r_j}$ ($j = 1, 2$) and

$$\frac{\langle r_1, \alpha_1 | P^2 | r_2, \alpha_2 \rangle}{\langle r_1, \alpha_1 | r_2, \alpha_2 \rangle} = \frac{2}{e^{2r_1} + e^{2r_2}} - \frac{4(\alpha_1 e^{r_1} - \alpha_2 e^{r_2})^2}{(e^{2r_1} + e^{2r_2})^2}. \quad (14)$$

Thus the calculated momentum variation is shown in Figs. 2(d) and 2(h). The squeezing effect is accurately captured by the DSS (10), and the accuracy can be attributed to the deformation of the constituent wave packets. Our variational solution illustrates well the phase-transition-like behavior for the $\Omega \rightarrow \infty$ regime.

Interestingly, the optimal variational parameters satisfy $\alpha_1 \approx -\alpha_2$ and $r_1 \approx r_2$ for $\Omega \gg 1$ [this is not the case for $\Omega \sim 1$; compare Figs. 3(b) and 3(c) with Figs. 3(e) and 3(f)]. In this case, the DSS in Eq. (10), which has been expressed in terms of the spin-oscillator hybrid mode b , takes a simple form (not normalized),

$$|\psi(r, \alpha, r, -\alpha, t)\rangle = (|r, \alpha\rangle + |r, -\alpha\rangle) \otimes |\downarrow\rangle + (1 - 2t)(|r, \alpha\rangle - |r, -\alpha\rangle) \otimes |\uparrow\rangle, \quad (15)$$

in terms of the original spin and oscillator mode. This form shows transparently the entanglement feature in the optimal wave function: For $g \ll 1$, $t \approx 1/2$ and the spin and oscillator is separable. As g increases, t decreases, which leads to

strong entanglement between spin and oscillator mode as shown in the insets in Figs. 2(b) and 2(f), and the overlap between $|\alpha\rangle$ and $|\alpha\rangle$ ($\alpha \sim \lambda$) gives a finite amount of squeezing.

Discussion. We have studied the spin-boson model (1) in the ultrastrong coupling limit by means of an effective classical potential and an improved variational wave function. We note that in the true adiabatic regime ($\Omega \gg 1$), the critical strength g for the entanglement coincides with the point where the squeezing effect is maximum. This coincidence can also be noticed from the crossover behavior of the effective classical potential (9). Nevertheless, the precise relation among the bifurcation in the classical potential in Fig. (1) or in the corresponding classical model [12], the squeezing effect, and the entanglement remains an interesting open problem in the ultrastrong coupling limit of the model (1).

This work was supported by NRF Grant No. 2009-0080453, the BK21 Program, the KIAS, and the APCTP.

-
- [1] J. M. Raimond, M. Brune, and S. Haroche, *Rev. Mod. Phys.* **73**, 565 (2001).
- [2] M. D. LaHaye, J. Suh, P. M. Echternach, K. C. Schwab, and M. L. Roukes, *Nature (London)* **459**, 960 (2009).
- [3] E. T. Jaynes and F. W. Cummings, *Proc. IEEE* **51**, 89 (1963).
- [4] H. P. Yuen, *Phys. Rev. A* **13**, 2226 (1976).
- [5] A. Zazunov, D. Feinberg, and T. Martin, *Phys. Rev. Lett.* **97**, 196801 (2006).
- [6] M.-J. Hwang, J.-H. Choi, and M.-S. Choi, *J. Phys.: Condens. Matter* **22**, 355301 (2010).
- [7] S. Ashhab and F. Nori, *Phys. Rev. A* **81**, 042311 (2010).
- [8] M. Devoret, S. Girvin, and R. Schoelkopf, *Ann. Phys.* **16**, 767 (2007).
- [9] J. Bourassa, J. M. Gambetta, A. A. Abdumalikov, O. Astafiev, Y. Nakamura, and A. Blais, *Phys. Rev. A* **80**, 032109 (2009).
- [10] D. Zueco, G. M. Reuther, S. Kohler, and P. Hänggi, *Phys. Rev. A* **80**, 033846 (2009).
- [11] G. Levine and V. N. Muthukumar, *Phys. Rev. B* **69**, 113203 (2004).
- [12] A. P. Hines, C. M. Dawson, R. H. McKenzie, and G. J. Milburn, *Phys. Rev. A* **70**, 022303 (2004).
- [13] G. Liberti, R. L. Zaffino, F. Piperno, and F. Plastina, *Phys. Rev. A* **73**, 032346 (2006).
- [14] C. P. Meaney, T. Duty, R. H. McKenzie, and G. J. Milburn, *Phys. Rev. A* **81**, 043805 (2010).
- [15] E. K. Irish, *Phys. Rev. Lett.* **99**, 173601 (2007).
- [16] F. Pan, X. Guan, Y. Wang, and J. P. Draayer, e-print arXiv:1004.2801.
- [17] H. Chen, Y.-M. Zhang, and X. Wu, *Phys. Rev. B* **40**, 11326 (1989).
- [18] H. B. Shore and L. M. Sander, *Phys. Rev. B* **7**, 4537 (1973).
- [19] J. Stolze and L. Müller, *Phys. Rev. B* **42**, 6704 (1990).
- [20] G. Benivegna and A. Messina, *Phys. Rev. A* **35**, 3313 (1987).
- [21] H. J. Spencer and S. Doniach, *Phys. Rev. Lett.* **18**, 994 (1967).
- [22] J. W. Negele and H. Orland, *Quantum Many-Particle Systems* (Addison-Wesley, Redwood, CA, 1988).
- [23] V. Coffman, J. Kundu, and W. K. Wootters, *Phys. Rev. A* **61**, 052306 (2000).
- [24] One may also use the recently proposed alternative methods in Refs. [15] and [16].
- [25] M. O. Scully and M. S. Zubairy, *Quantum Optics* (Cambridge University Press, Cambridge, 1997).